Pharmaceutical Research, Vol. 25, No. 1, January 2008 (© 2007)
DOI: 10.1007/s11095-007-9417-y

Research Paper

Effect of Stabilizer on the Maximum Degree and Extent of Supersaturation and Oral Absorption of Tacrolimus Made By Ultra-Rapid Freezing

Kirk A. Overhoff,[1] Jason T. McConville,[1] Wei Yang,[1] Keith P. Johnston,[2,4] Jay I. Peters,[3] and Robert O. Williams III[1]

Received April 24, 2007; accepted July 18, 2007; published online October 30, 2007

Purpose. Solid dispersions containing various stabilizers and tacrolimus (TAC) prepared by an Ultra-rapid Freezing (URF) process were investigated to determine the effect on their ability to form supersaturated solutions in aqueous media and on enhancing transport across biological membranes.
Materials and Methods. The stabilizers included poly(vinyl alcohol; PVA), poloxamer 407 (P407), and sodium dodecyl sulfate (SDS). *In vivo* absorption enhancement in rats was also investigated. Dissolution studies were conducted at supersaturated conditions in both acidic media for 24 h and at delayed release (enteric) conditions to simulate intestinal transit.
Results. The rank order of C/Ceq_{max} in the dissolution studies at acidic conditions was URF-P407>URF-SDS>Prograf® (PRO)>URF-PVA:P407. For C/Ceq_{max} under enteric conditions, the order was URF-SDS>PRO>URF-PVA:P407>URF-P407, and for the extent of supersaturation (AUC) in acidic and pH shift conditions it was URF-SDS>PRO>URF-PVA:P407>URF-P407. The pharmacokinetic data suggests URF-P407 had the greatest absorption having higher C_{max} with a 1.5-fold increase in AUC compared to PRO. All URF compositions had a shorter T_{max} compared to PRO.
Conclusions. The nanostructured powders containing various stabilizing polymers formed by the URF process offer enhanced supersaturation characteristics leading to increased oral absorption of TAC.

KEY WORDS: amorphous; *in vitro–in vivo* correlation; nanoparticle; particle engineering; rapid freezing; supersaturation; tacrolimus.

INTRODUCTION

Tacrolimus (TAC) is a hydrophobic macrolide antibiotic (MW 822.1 kDa) that has shown promise as a potent immunosuppressive agent (1). Clinical and pharmacokinetic studies revealed that TAC may have superior immunosuppressive properties compared to cyclosporine A (CsA), but similar erratic absorption properties have limited its potential (2–4). Mean oral bioavailability is reported to be 25% and ranges from 4 to 93% (5,6). Various strategies have been employed to increase the bioavailability of TAC including compounding TAC as an oral liquid (7), solid dispersions (8), complexation with cyclodextrins (9,10), and incorporation into liposomes for oral (11,12) and pulmonary (13) delivery.

The formation of a supersaturated state with solid dispersions and solid solutions may increase oral bioavailability of active pharmaceutical ingredients (APIs) which suffer from poor/erratic bioavailability. In fact, it was proposed that increasing the solubility greater than twofold through polymorphism can have a significant increase in biopharmaceutical activity (14–16). Mechanistically speaking, APIs in a polymorph with a higher thermodynamic activity form a supersaturated solution with a apparent solubility above the equilibrium solubility and therefore have an increased driving force for transport across biological membranes such as the epithelial membrane within the GI tract (17). Another challenge, however, is to maintain the supersaturated state and prevent precipitation of the API out of solution. Stabilizing polymers such as hydroxypropylmethyl cellulose (HPMC), which are known to form hydrogen bonds with the API preventing precipitation (18,19), can be incorporated into the composition. HPMC and polyvinylpyrrolidone (PVP) have been shown to be two of the best polymers for maintaining supersaturation of poorly water soluble APIs by preventing precipitation of the API into solution. However, the ability of other polymers/surfactants to stabilize supersaturated solutions and prevent precipitation is largely unknown.

Rapid freezing processes such as the Spray Freezing into Liquid (SFL; 20–22) and Ultra-rapid Freezing (URF; 23,24) have been shown to produce particles with enhanced dissolution rates for biopharmaceutical classification system (BCS) class II active pharmaceutical ingredients (API).

[1] College of Pharmacy, University of Texas at Austin, Mailstop A1920, Austin, Texas 78712-1074, USA.
[2] Department of Chemical Engineering, University of Texas at Austin, Austin, Texas 78712, USA.
[3] Department of Medicine, Division of Pulmonary Diseases/Critical Care Medicine, University of Texas Health Science Center at San Antonio, San Antonio, Texas 78229, USA.
[4] To whom correspondence should be addressed. (e-mail: kpj@che.utexas.edu)

Recently, *in vivo* studies have shown that nanostructured danazol particles produced from SFL have increased oral absorption in mice (21) and nanostructured itraconazole particles from SFL have improved both oral and pulmonary absorption in mice compared to the commercial product (25). The URF process utilizes a cryogenic surface to rapidly freeze the API/polymer solution to produce nanostructured powders characterized by their high surface area, increased wettability, amorphous API structure, and rapid dissolution rates. Briefly, the process involves freezing an API/polymer solution directly onto the surface of a cryogenic substrate with a thermal conductivity k between 10 and 20 W/(m×K), collecting the frozen particles and removing the solvent via lyophilization.

However, determining an *in vitro–in vivo* correlation with amorphous particles can be problematic as supersaturation levels in the GI tract may not correlate with levels in the dissolution vessel. Premature precipitation of the active following oral administration can decrease the overall absorption of the API by decreasing the driving force for transport across the biological membrane and limiting the time available for absorption. Although the mechanism for inhibition of recrystallization in supersaturated solutions has not been established (26), it is believed that adsorption of polymer onto the hydrophobic surface of crystals inhibit growth of embryo that nucleate from metastable solutions (27) and suspensions (28). Recently, Raghaven *et al.* (18,29) have proposed hydrogen-bonding as a mechanism to inhibit or retard crystal growth of hydrocortisone acetate in supersaturated solutions containing HPMC. Therefore, inclusion of polymers such as HPMC and PVP which have a number of hydrogen-bonding acceptor and donor sites have been shown to maintain supersaturation of TAC, hydrocortisone acetate, and an experimental poorly water soluble compound RS-8359 for up to 24 h (8,19,30). However, the effectiveness of the polymer stabilizer is API dependent as illustrated for HPMC, which is known to maintain a supersaturated solution of hydrocortisone acetate for up to 72 h. However the supersaturation of an oestradiol solution decreased 60% after only 6 h (26).

The objective of this study was to assess the effects of combinations of stabilizers on the maximum degree and extent of supersaturation of TAC, and attempt to establish if an *in vitro–in vivo* correlation exists between supersaturation and improved pharmacokinetic parameters for orally dosed TAC. The selected polymers were partially hydrolyzed polyvinyl(alcohol; PVA) which has been shown to increase drug concentration *in vivo* (31) and poloxamer 407 (P407) which has been shown to alter surface properties of crystals (32). Sodium dodecyl sulfate (SDS), a non-polymeric anionic surfactant, may be expected to facilitate wetting and dissolution rates, but supersaturation of pharmaceuticals with SDS has not been reported below the critical micelle concentration. TAC/excipient particles were manufactured using the Ultra-rapid Freezing Process (URF) and the physico-chemical properties were compared with those of the bulk API, as well as the commercially available amorphous solid dispersion of TAC and HPMC (33). Maximum *in vitro* supersaturation levels (C/Ceq_{max}), defined as the ratio of the highest instantaneous TAC concentration (C) to the equilibrium solubility of crystalline TAC (Ceq), and extent of supersaturation defined as the total supersaturation over time, measured by the area under the supersaturation curve (AUC). These properties were used to assess the performance of the URF compositions in both acidic media (for 24 h) and under shifting pH conditions defined in the US Pharmacopoeia. Pharmacokinetic analysis of orally administered TAC compositions in a single dose study design was conducted to determine the performance of the compositions.

MATERIALS AND METHODS

Materials

Bulk tacrolimus (TAC) and Prograf® (PRO) capsules (5 and 1 mg, Fujisawa) were generously donated by the Dow Chemical Company (Midland, MI, USA). Poly(vinyl) alcohol (PVA, Mw 13,000–23,000, 87–89% hydrolyzed) and sodium dodecyl sulfate (SDS) were purchased from Sigma-Aldrich (St. Louis, MO, USA). Poloxamer 407 [(P407), Mw 9,800–14,600] was purchased from Spectrum Chemicals (Gardena, CA, USA). Sodium phosphate tribasic (Na_3PO_4) was purchased from Fisher Scientific chemicals (Fair Lawn, NJ, USA). High performance liquid chromatography (HPLC) grade acetonitrile (ACN) was obtained from EM Science (Gibbstown, NJ, USA).

Methods

Preparation of the URF Micronized Powders

The URF compositions investigated in this study are described in Table II. The compositions were prepared by dissolving TAC and hydrophilic excipients at a 1:1 API/excipient ratio and 1.0% solids in a 60/40 mixture of ACN and water. The TAC/excipient feed solutions were processed using the URF apparatus. The feed solutions were applied to a cryogenic substrate cooled to a temperature of −150°C, collected, and lyophilized using a VirTis Advantage benchtop tray lyophilizer (The VirTis Company, Inc. Gardiner, NY, USA). Micronized powders were stored at room temperature and under desiccant until characterized.

Scanning Electron Microscopy (SEM)

The powder samples were sputter coated using a K575 sputter coater (Emitech Products, Inc., Houston, TX, USA) with gold-palladium for 35 s and viewed using a Hitachi S-4500 field emission scanning electron microscope (Hitachi High Technologies Corp., Tokyo, Japan). An accelerating voltage of 5–10 kV was used to view the images. All SEM fields of view were representative of the entire sample.

Supersaturated Dissolution Testing Under Acidic Conditions

Supersaturated dissolution testing was carried out on PRO and all URF micronized powder samples using a small volume dissolution apparatus equipped with a paddle stirring mechanism (VanKel VK6010 Dissolution Tester with a Vanderkamp VK650A heater/circulator, Varian Inc., Cary, NC, USA). The small volume vessels were filled with 100 ml of deaerated (via He sparge) 0.2% NaCl in 0.1N HCl

(Japanese Pharmacopeia XIX, JP first media) and heated and maintained at 37.0±0.2°C throughout the dissolution study. Amounts of drug compositions were weighed out corresponding to 28× the aqueous solubility of TAC (7 mg TAC/vessel) and added to the vessels. The paddle speed was set to 200 RPM and a 3 ml aliquot of sample was taken manually at 10, 20, 30, 60, 120, 240, and 1,440 min, with no medium replacement. This aliquot was filtered first through a 0.45 μm GHP Acrodisc syringe filter (Pall, East Hills, NY, USA) and then through a 0.02 μm Whatman Anotop 25 membrane filter (Maidstone, UK). A 0.75 ml portion of the filtered solution was transferred to a 1.5 ml HPLC vial and diluted with 0.75 ml ethanol, vortexed and analyzed using a modified method developed by Nishikawa *et al.* (34). A Shimadzu LC-10 liquid chromatograph (Shimadzu Corporation, Kyoto, Japan) equipped with an Alltech Inertsil ODS-2 5 μm C_{18} column (Alltech Associates, Inc., Deerfield, IL, USA) maintained at 60°C was used to quantitate the TAC. A 70:30 ACN/water mobile phase at 0.9 ml/min eluted the TAC peak at 8.5 min. The maximum absorbance was measured at wavelength λ=214 nm. System suitability requirements were met ($R^2 \geq 0.999$, precision ≤2.0% RSD).

Supersaturated Dissolution Testing Under pH Shift Conditions

All dissolution conditions were maintained as described above except that the dissolution medium was changed during the dissolution test. Using the USP enteric test (method A) conditions as a guide, 75 ml of 0.1 N HCl was added to the small volume dissolution vessels and heated to 37.0±0.2°C. All dissolution media was deaerated via He sparge. Sample powders were added to the vessels stirred at 200 RPM. After 2 h, 21 ml of 0.2 M Na_3PO_4 (1:3 v/v buffer/acid ratio observed) was added to increase the pH to 6.8 for the remainder of the study. Sample were taken at the following time points: 15, 30, 60, 120, 135, 150, 240, and 1,440 min; then the samples were filtered, diluted, and analyzed by HPLC as stated above.

X-ray Powder Diffraction (XRD)

The X-ray diffraction pattern of all powder samples were analyzed using a Philips 1710 X-ray diffractometer with a copper target and nickel filter (Philips Electronic Instruments, Inc., Mahwah, NJ, USA). The leveled powder was measured from 5 to 45 2θ degrees using a step size of 0.05 2θ degrees and a dwell time of 1 s.

Surface Area Analysis

Specific surface area was measured using a Nova 2000 v.6.11 instrument (Quantachrome Instruments, Boynton Beach, FL, USA). Weighed powder was added to a 12 mm Quantachrome bulb sample cell and degassed for a minimum of 3 h. The sample was then analyzed (n=3) by the NOVA Enhanced Data Reduction Software v. 2.13 via the Brunauer, Emmett, and Teller theory of surface area (35).

In Vivo Oral Absorption Studies

An animal study was designed and approved by the University of Texas at Austin Institute of Animal Care and Use Committee (IACUC). Four groups of six pre-catheterized male Sprague–Dawley rats (300 g) were dosed with 5 mg/kg tacrolimus in size 9 gelatin capsules (Torpac Inc., Fairfield, NJ, USA) followed by administration of 0.4 ml water via oral gavage. An aliquot of 300 μl of blood was withdrawn at 0.5, 1, 1.5, 2, 3, 4, 6, and 24 h and replaced with 6 units/μl heparinized normal saline solution. Fifty microliters of the whole blood sample was analyzed by the PRO-Trac™ II FK-506 ELISA assay (Diasorin Inc., Stillwater, MN) to quantitate amount of tacrolimus (36). Whole blood samples were diluted when necessary with the calibrator 0 provided with the PRO-Trac™ kit in order to fit within the specified standard curve range (0.3–30 ng/ml). Pharmaco-kinetic parameters were determined using a non-compartmental analysis in WinNonlin Professional version 2.1 (Pharsight Corporation, Mountain View, CA, USA).

Statistical Analysis

One-way analysis of variance (ANOVA, α=0.05) was used to determine statistically significant differences between results. Results with p values<0.05 were considered statistically significant. Post hoc analysis using Tukey's honestly significant difference (HSD) test was performed after analysis to determine individual differences between compositions. Mean differences greater than the HSD were deemed statistically significant.

RESULTS

In vitro Characterization of URF Micronized Powders

The URF process was used to manufacture compositions of TAC listed in Table I. The micronized powders were analyzed using SEM to observe the surface morphology. Bulk TAC in Fig. 1a displays a plate-like shape with particle sizes ranging from a few microns to over 120 μm in diameter. The particle surfaces of the bulk TAC appear to be smooth with few pores. In contrast, the URF micronized powders (Fig 1b–d), are a highly porous network of nanostructured aggregates. URF-SDS powder (Fig. 1b) is composed of discrete nanoparticles measuring less than 200 nm in diameter. URF-PVA:P407 powder (Fig. 1c) appears to be a

Table I. Tacrolimus Compositions Produced using the URF Process

URF Composition	Active (A)	Excipient (E1:E2)	Ratio (A:E1:E2)	Percent of Total Solids
URF A	TAC	SDS	1:1	1.00
URF B	TAC	PVA:P407	1:0.5:0.5	1.00
URF C	TAC	P407	1:1	1.00

combination of agglomerated or fused nanoparticles with smoothed edges. The size of the agglomerates appear to be larger than those in Fig. 1a but still composed of nanoparticles appearing to be less than 1 μm in diameter. Lastly, URF-P407, (Fig. 1d) appears to have few submicron domains. A magnified view reveals large agglomerated nanoparticles which have fused to create a porous macrostructure.

Figure 2 shows the XRD results for bulk TAC which has a characteristic doublet peak at 19.10 and 19.95 2θ degrees and a secondary crystalline peak at 23.45 2θ degrees. All compositions of the URF micronized powders lack any characteristic crystalline peaks of TAC. URF-P407 contains two crystalline peaks at 19.4 and 23.6 2θ degrees and is associated with the P407 in the composition, which is partially crystalline after lyophilization as has been observed in rapidly frozen or melt compositions (20,37,38). Likewise, these two peaks are seen to a lesser degree in the URF-PVA:P407 composition due to a decrease in P407 in the composition. It is noted that these diffraction patterns in Fig. 2 were collected prior to dosing *in vivo* and represent samples under storage conditions at room temperature and low moisture (20% relative humidity) for up to 1 year.

In vitro supersaturation dissolution studies were conducted in acidic media for 24 h for each of the URF micronized powders, as well as the control, the PRO powder, as shown in Fig. 3 and summarized in Table III. Sample powders were added to the dissolution media at approximately 28-times the equilibrium solubility of TAC in the media as measured by HPLC. The degree of supersaturation is defined as the concentration (C) of TAC in the media divided by the equilibrium solubility (Ceq) of crystalline TAC within the medium, C/C_{eq}. All URF micronized powders had rapid dissolution rates reaching their maximum supersaturation within 2 h. URF-SDS displayed a high C/Ceq_{max} with an extended supersaturation that produced the highest AUC of all compositions investigated. URF-PVA:P407 displayed the lowest C/Ceq_{max} at 14.5-times equilibrium solubility, and precipitated out to 3.5-times equilibrium solubility after 24 h. URF-P407 had the fastest

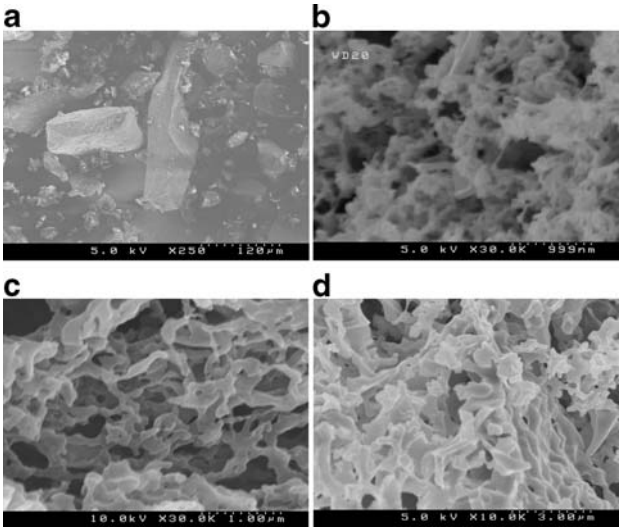

Fig. 1. SEM micrographs of Bulk TAC (**a**), URF-SDS (**b**), URF-PVA:P407 (**c**), URF-P407 (**d**).

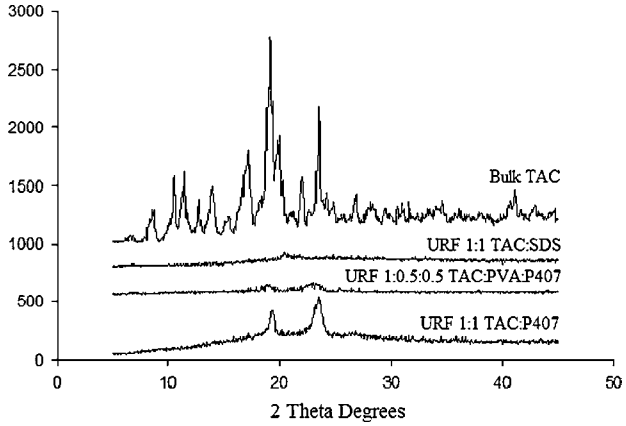

Fig. 2. X-ray powder diffraction of amorphous TAC compositions prepared using the URF freezing process.

dissolution rate and the highest maximum supersaturation of all powders examined with a C/C_{eq} of 22.8-times equilibrium solubility at 1 h. However, URF-P407 rapidly precipitates to 6.3-times equilibrium solubility at 6 h and was the only one of the three URF processed powders investigated to reach equilibrium solubility at 24 h. PRO powder, which is composed of equal ratios of amorphous TAC and HPMC (33), showed a slower dissolution rate reaching its maximum supersaturation level (17-times) after 6 h. However, for PRO TAC, a supersaturation at 11-times equilibrium solubility was still present after 24 h.

Because the powders were to be administered orally, supersaturated dissolution was also investigated using an enteric dissolution test method to more accurately represent the pH conditions encountered during transit from the acidic environment in the stomach to the basic environment in the upper small intestine (Fig. 4; parameter summary in Table III). TAC is known to have pH independent solubility over the pH range 1–9 (39) and therefore has the same solubility in acidic media as in the pH 6.8 buffer (2.2 μg/ml; 8). Upon a pH shift from pH 1.2 to 6.8 at 2 h, URF-SDS was the only composition with an increase in supersaturation level reaching its C/Ceq_{max} 15 min after the pH shift occurred. After 15 min, TAC precipitated out from solution and after 24 h had two-times equilibrium solubility in the basic dissolution media. Both URF-PVA:P407 and URF-P407 had similar supersaturation profiles reaching their maximum supersaturation before precipitation occurred. PRO, however, began to precipitate out of solution immediately after the pH shift occurred. As a result of the pH shift, PRO was not able to achieve the level of supersaturation observed in the acidic media. After the pH shift occurred, a high level of supersaturation was not maintained. PRO precipitated to only 2.5-times equilibrium solubility after 24 h, unlike the case in acid conditions where supersaturation was extended at high levels.

Both URF-SDS and URF-P407 had significantly higher ($p<0.05$) maximum supersaturation ratios (C/Ceq_{max}) in acidic medium while only URF-SDS had a significantly higher ($p<0.05$) C/Ceq_{max} when tested with the pH shift dissolution conditions. The URF micronized powders reached their C/Ceq_{max} within 1–2 h in acidic media while PRO reached its C/Ceq_{max} at 6 h. All URF compositions

reached their C/Ceq_{max} before PRO under acidic conditions indicating the rapid wetting that occurs with URF micronized powders. However, both URF-PVA:P407 and URF-P407 had lower extents of supersaturation (AUC) compared to PRO, while URF-SDS had better AUC than PRO under acidic and pH shift conditions, respectively.

In vivo Characterization of URF Micronized Powders

Whole blood samples were analyzed using a commercially available immuno-assay kit and the TAC whole blood concentrations *vs.* time are plotted in Fig. 5. The absorption profiles for the URF compositions indicate faster absorption and higher TAC blood levels during the absorption phase. From these profiles, non-compartmental analysis, as discussed by Arima *et al.* (10), was performed to determine the appropriate pharmacokinetic parameters for each of the compositions tested and are summarized in Table IV. One-way ANOVA analysis revealed that there were significant differences ($p<0.05$) between the four compositions in regards to C_{max} and T_{max} while there were no statistical differences ($p>0.05$) regarding the tacrolimus half-life ($T_{1/2}$), the elimination rate constant (K_{el}), or the AUC. All URF micronized powders had higher C_{max} values ranging from 65.2 to 138.5 ng/ml as compared to the PRO powder which had a C_{max} of 51.5 ng/ml. However, only URF-P407 powder had a significantly higher C_{max} compared to PRO while URF-SDS and PVA:P407 powders were not statistically different ($p>0.05$). The measured T_{max} for each URF micronized powder was between 0.5 and 0.67 h while the PRO powder had a measured T_{max} of 1.3 h. All powders had similar K_{el} while PRO had the lowest at 0.094 h^{-1} and URF-P407 had the highest K_{el} at 0.106 h^{-1}. Consequently, URF-P407 had the fastest clearance of TAC and therefore had the fastest half-life at $T_{1/2}$=6.9 h. URF-P407 had the highest $AUC_{(0-24)}$ at 450.6 ng×h/ml. Despite having a 1.5-fold increase in AUC compared to PRO, this was not statistically significant ($p>0.05$). URF-PVA:P407 had the second highest AUC value at 319.8 ng×h/ml followed by PRO at 298.8 ng×h/ml. URF-SDS had the lowest AUC at 223.6 ng×h/ml. Therefore, the pharmacokinetic parameters assessed in the study showed enhanced absorption by the URF compositions (C_{max}, T_{max}) as compared to PRO while elimination rate constants and AUCs were enhanced in most compositions.

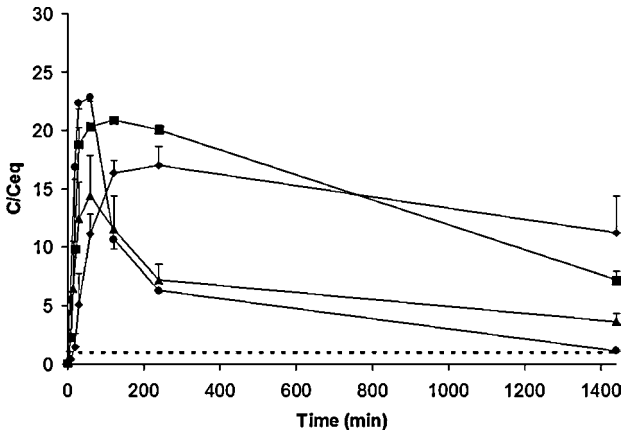

Fig. 3. Supersaturated dissolution of tacrolimus in acidic dissolution medium: URFSDS (*filled square*), URF-PVA:P407 (*filled triangle*), URF-P407 (*filled circle*), PRO capsule powder (*filled diamond*), tacrolimus equilibrium solubility (*broken lines*).

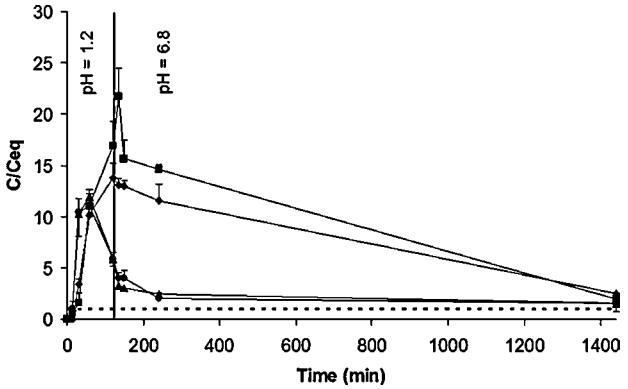

Fig. 4. Supersaturated dissolution of tacrolimus under enteric conditions: URF-SDS (*filled square*), URF-PVA:P407 (*filled triangle*), URF-P407 (*filled circle*), PRO capsule powder (*filled diamond*), tacrolimus equilibrium solubility (*broken lines*).

DISCUSSION

In the present study, nanostructured aggregate powders containing TAC and excipients, manufactured by the URF process were characterized in order to better understand the mechanism of supersaturation stabilization. Furthermore, an attempt is made to identify the effect of supersaturation on increasing the bioavailability of TAC. *In vitro* characterization of the URF micronized powders revealed that they were composed of nanoparticle domains containing amorphous TAC. URF-P407 displayed the lowest surface area. Similar results were reported by Hu *et al.* (20) who produced binary mixtures containing danazol and a hydrophilic polymer by another cryogenic process SFL. The surface area of danazol:P407 was 5.5 m^2/g, while danazol:PEG and danazol:PVP powders had surface areas of 12.0 and 89.8 m^2/g, respectively.

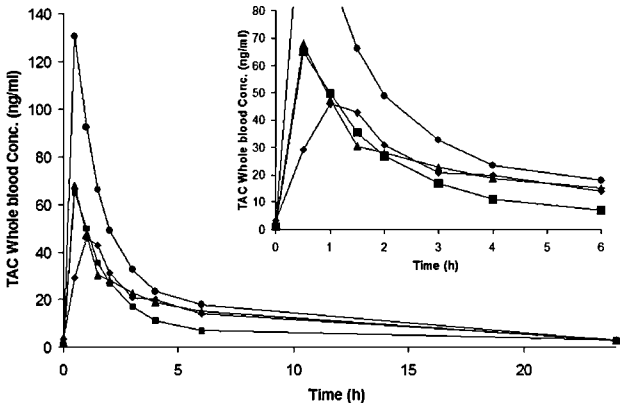

Fig. 5. Mean whole blood absorption levels of TAC compositions produced using the URF process compared to the commercially available tacrolimus product. Powders were given an gelatin capsule containing 1.5 mg equivalent TAC (5 mg/kg) dosed via oral gavage to a rat model: URF-SDS (*filled square*), URF-PVA:P407 (*filled triangle*), URF-P407 (*filled circle*), PRO (*filled diamond*).

Table II. Specific Surface Area of URF Processed Compositions

Composition	Surface Area (m^2/g)
URF A	54.96
URF B	43.68
URF C	7.73
Bulk TAC	0.53

In a similar study by McConville *et al.* (38) low surface areas were attributed to incorporation of high levels (>30%) of a liquid surfactant, polysorbate 20. It was hypothesized that surface area reduction occurred during the lyophilization process. During lyophilization, compositions containing excipients, which exist in a liquid state at ambient conditions, have more molecular mobility than those containing solid excipients with high glass transition temperatures (e.g. PVP). With the greater mobility, the particles may coalesce to reduce the surface area, as has been observed for polysorbate 20. However, all polymers used in this study are solids at room temperature and should provide greater rigidity compared to liquid surfactants during lyophilization and gave much higher surface areas than polysorbate 20 (38). The modestly lower surface area for P407, relative to the other formulations in Table II, may reflect its much lower T_g.

In the case of TAC, Yamashita *et al.* (8) investigated the performance of HPMC, PVP, and polyethylene glycol (PEG) on maintaining the supersaturation of TAC. While all samples had reached the same C/Ceq_{max}, only HPMC was able to maintain at least 95% of the maximum supersaturation over 24 h in acidic medium. To date, the mechanism by which they maintain supersaturation of dissolved drug has not been delineated.

Apart from their particle formation properties, polymers also play an important role in enhancing dissolution rates through wettability, and at supersaturated conditions, maintaining API supersaturation. Both SDS and P407 are known to increase wetting due to their high hydrophilic–lipophilic balance (HLB) values, while PVA is used as a stabilizing agent and has been reported to enhance supersaturation. Suzukiand and Sunada (31) report that although PVA maintained supersaturation to a lesser degree than HPMC or PVP, dissolution supersaturation was enhanced by more than 20-times compared to the crystalline API. The present supersaturation studies indicate that P407 is not able to maintain supersaturation for extended periods of time of up to 24 h, but the enhanced wetting properties of the polymer allow for high supersaturation levels at short times. Inclusion of PVA into the composition decreases the level of supersaturation but allows for slightly slower precipitation rates in the acidic media after 6 h. SDS, although not a polymer, was able to maintain supersaturation of TAC at a similar level to HPMC under both supersaturated dissolution conditions tested. It is important to note that the concentrations of SDS present in the medium reached only 10% of the critical micelle concentration in aqueous media (conc. SDS_{disso}= 2.5×10^{-4} M and $SDS_{CMC}=2.8\times10^{-3}$ M) containing a salt as calculated by Dutkiewicz and Jakubowska (40). SDS dissociates in the electrolyte medium to produce a hydrogen-bonding acceptor site. The interaction between the hydrophobic tail of a surfactant molecule and the hydrophobic surface of the API molecule, and a second complimentary interaction between the sulfate group of the surfactant molecule with an adjacent hydrogen bonding donor site on the API may facilitate solvation of the drug in water. The same type of mechanism may take place for the polymeric stabilizers with hydrophobic moieties and hydrogen bonding sites. Furthermore, it is likely that, other SDS molecules will adsorb with tails oriented onto the surface of embryo crystals of TAC with the head groups extending into water. The anionic sulfate groups on the adsorbed surfactant will provide electrostatic repulsion inhibiting particle growth from coagulation.

In solution, the polymers may adsorb onto the surface of small embryo particles and inhibit crystal growth by blocking active surface and providing steric stabilization. In addition, hydrogen bonding between TAC and the stabilizers may compliment hydrophobic interactions between these species to help maintain supersaturation. Structurally, HPMC has many hydroxyl groups which are both hydrogen bond donors and acceptors for the TAC. Investigation of the TAC structure (Fig. 6) reveals four possible H-bond acceptor sites indicated by circles along with three possible donor sites indicated by triangles. PVA has one H-bond donor and acceptor per monomer unit while P407, on the other hand, has one donor site per polymer unit.

PRO maintained supersaturation under acidic conditions to a similar extent as SDS, as shown in Table III. The less effective stabilization by PVA and P407 may reflect weaker adsorption on the surfaces of the embryo particles and thus less steric stabilization against particle growth. In addition P407 with only one H-bonding donor sight per chain may not have interacted strongly enough with hydrogen bond acceptor sites on TAC to inhibit crystallization. PVA:P407 was slightly better than P407 alone, perhaps indicating that the addition of hydrogen bond donor sites in PVA provided beneficial interactions with TAC.

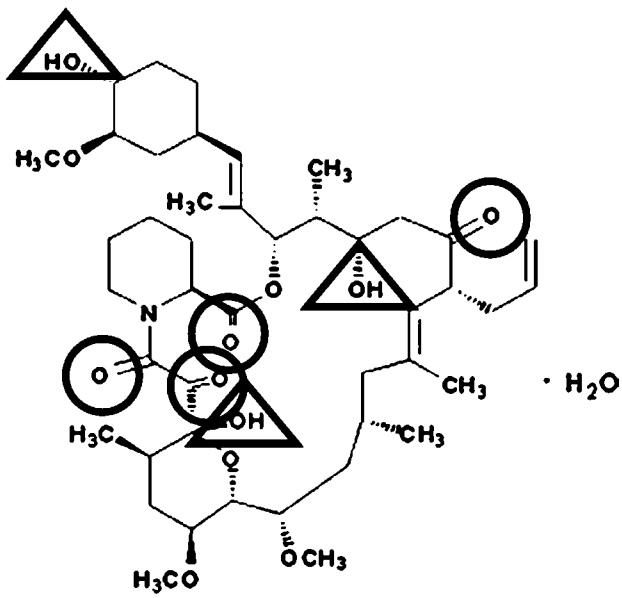

Fig. 6. Possible hydrogen-bonding sites for tacrolimus: hydrogen-bond donor (*open triangle*), hydrogen-bond acceptor (*open circle*).

Table III. AUC Ratios of URF Processed Compositions Compared to PROGRAF

Composition	Ratio to PROGRAF (Acid)	Ratio to PROGRAF (pH Shift)
URF A	1.042	1.184
URF B	0.448	0.335
URF C	0.376	0.320
Prograf®	1.000	1.000

The shift in media pH at 2 h during the supersaturation dissolution studies dramatically affected the physical stability of the supersaturated solutions. Again the solubility of the API in aqueous media without stabilizers is independent of pH. While URF-PVA:P407 and URF-P407 began precipitating before the pH shift occurred the PRO composition immediately began precipitating after the pH was increased. This precipitation may produce a loss in bioavailability as a result of decreased absorption in the small intestine. Interestingly, the degree of supersaturation for URF-SDS increased for at least 15 min after the pH shift occurred before it then decreased. However, the rate of precipitation out of solution over the next 21h was much more pronounced than under acidic conditions in Fig. 3 indicated by the supersaturation level at 24 h. This trend was seen for all compositions investigated at pH 6.8 compared to the acidic media and could be the result of bonding strength changes from the presence of inorganic salts. Khutoryanskiy *et al.* (41) suggests that the presence of inorganic salts such as Na_3PO_4 (in particular, the divalent and trivalent phosphates) in the dissolution media can alter the ionic strength or thermodynamic properties of the solution and salt out the API. Introduction of inorganic salts can cause collapse of the polymer chains on the surface of embryo API particles. This collapse will weaken steric stabilization and may lead to precipitation of the API out of solution, particularly with P407 in the presence of NaCl and Na_3PO_4 (42).

Both the acidic and enteric *in vitro* supersaturation test condition studies reveal that the URF micronized powders rapidly wet and dissolve resulting in solutions with high C/Ceq_{max}. The *in vivo* absorption profiles also indicate rapid wetting and dissolution as evidenced by the rapid T_{max} for all URF compositions leading to rapid absorption times. This rapid dissolution could be a combination of both the polymer characteristics (i.e. wetting enhancement) as well as the URF technology which create amorphous nanoparticle domains of API. Because the powders were dosed within a size #9 hard gelatin capsule by oral gavage, the powders were not prewetted by aqueous solution containing a surfactant. Therefore, the powders must rely on the gastric fluid and on the enhanced powder wetting properties (i.e. polymer/surfactant wettability, and available surface area) to wet, disintegrate, and dissolve the particles. It is clear from both the *in vitro* and *in vivo* data that the URF micronized powders are wetted more effectively than PRO leading to enhanced absorption profiles early in the absorption phase. While numerous studies have reported increases in bioavailability as a result of API being in a supersaturated state, rapid dissolution and supersaturation could prove counter productive, especially for examples in which the API can precipitate during transit when the pH increases from the stomach to upper small intestine. Absorption of the API can be compromised in instances when all of the powder is dissolved in the stomach but not fully absorbed through the stomach lining. As the API moves into the upper small intestine, the solution begins to precipitate arresting absorption. While it is true that the measured pharmacokinetic parameters for the URF micronized powders were superior to those of PRO, premature precipitation while in transit could have prevented the powders from achieving their full potential. This is evidenced by URF-P407 which showed a high C/Ceq_{max} *in vitro* under acidic conditions and also had the highest C_{max} *in vivo*. In this case, URF-P407 probably completely dissolved into a supersaturated solution leading to excellent absorption within the stomach lining.

Absorption of TAC within the small intestine is also affected by a number of biological processes making further *in vitro–in vivo* correlations difficult. TAC is reported as a substrate for p-glycoprotein (P-gp), a plasma protein involved with efflux pumps and responsible for multi-drug resistance (43). In addition, TAC is known to degrade enzymatically within the GI lining from CYP3A metabolic enzymes further lowering its absorption potential. However, recent studies have suggested that within the rat and mouse small intestine, the CYP3A enzymes play a larger role in limiting TAC absorption rather than P-gp as previously thought (44–46). Saitoh *et al.* (47) showed via an in situ intestinal loop technique that when TAC was administered with a specific CYP3A inhibitor (clotrimazole) the TAC AUC increased seven fold. Lastly, Kagayama *et al.* (48) showed that rats receiving TAC in a fasted state can have twice the AUC of rats who received the same dose of TAC in a fed state. Because these barriers to TAC absorption are well documented in rats (48) and because there is a fair correlation between mammal species regarding intestinal absorption (49), this animal model is valid for preliminary pharmacokinetic analysis of the URF micronized compositions containing TAC.

Table IV. Pharmacokinetic Parameters for URF Processed Compositions and the Commercially Available Tacrolimus Product

Composition	C_{max} (ng/ml)	T_{max} (h)	$T_{1/2}$ (h)	K_{el} (h^{-1})	AUC (0–24) (ng×h/ml)	AUC (inf) (ng×h/ml)
URF-SDS	65.2±43.4	0.67±0.41	7.5±1.8	0.096±0.02	223.6±102.7	254.8±113.3
URF-PVA:P407	67.9±11.7	0.5±0.0	7.5±1.4	0.095±0.02	319.8±138.2	348.6±141.4
URF-P407	138.5±69.1	0.6±0.2	6.9±2.3	0.106±0.03	450.6±188.1	476.1±187.1
Prograf®	51.5±19.8	1.3±0.4	7.7±1.8	0.094±0.02	298.8±83.2	330.2±84.9

AUC Area under the curve

CONCLUSION

The relationship between supersaturation behavior, measured during dissolution, and *in vivo* absorption enhancement was investigated for various compositions of TAC prepared by the URF process. The ability of two polymers, PVA and P407, and one low molecular weight surfactant, SDS, to provide sufficient supersaturation levels (C/Ceq_{max}) and to maintain supersaturation under acidic and pH shifted conditions was determined. The supersaturation for URF-SDS was equal to or better than PRO under acidic and pH shift conditions, respectively. The levels of SDS were well below the CMC in the medium. It is hypothesized that SDS was able to maintain supersaturation of TAC through adsorption onto the surface of tiny embryo particles to inhibit growth and precipitation. For URF-PVA:P407 and URF-P407, AUC and maintenance of supersaturation were poorer than for PRO. URF-P407 was the only composition where the concentration decayed to the equilibrium value after 24 h in acidic medium. Under pH shifted conditions, URF-SDS was the only composition that did not precipitate immediately after a shift in pH. URF-PVA:P407 and URF-P407 both began to precipitate while still in acid, while PRO began to precipitate immediately after the shift. Although TAC solubility and chemical stability are independent of pH, the rate of precipitation was more extensive in basic than in acidic media possibly as the result of changes caused by the presence of inorganic salts in the buffer. *In vivo* results in a rat model reveal enhanced C_{max} and T_{max} for all URF micronized compositions and higher AUC in URF-PVA:P407 and URF-P407 resulting from enhanced dissolution properties (e.g. rapid onset of supersaturation) of the processed powders. Based on the pharmacokinetic parameters and supporting *in vitro* supersaturation data, it is concluded that the enhanced physico-chemical properties of URF micronized powders led to enhanced *in vivo* absorption over PRO (Table IV).

ACKNOWLEDGEMENTS

The authors kindly acknowledge the financial support from The Dow Chemical Company. Kirk A. Overhoff is a continuing American Fellowship for Pharmaceutical Education (AFPE) Fellow from 2004 to 2006 and a 2005–2006 University Continuing Fellowship recipient. In addition, the authors would like to gratefully thank Dr. Nathan Wiederhold at the University of Texas Health Science Center for lending his expertise regarding the ELISA analysis.

REFERENCES

1. D. H. Peters, A. Fitton, G. L. Plosker, and D. Faulds. Tacrolimus—a review of its pharmacology, and therapeutic potential in hepatic and renal-transplantation. *Drugs* **46**:746–794 (1993).
2. W. J. Jusko, W. Piekoszewski, G. B. Klintmalm, M. S. Shaefer, M. F. Hebert, A. A. Piergies, C. C. Lee, P. Schechter, and Q. A. Mekki. Pharmacokinetics of tacrolimus in liver-transplant patients. *Clin. Pharmacol. Ther.* **57**:281–290 (1995).
3. A. Lampen, U. Christians, F. P. Guengerich, P. B. Watkins, J. C. Kolars, A. Bader, A. K. Gonschior, H. Dralle, I. Hackbarth, and K. F. Sewing. Metabolism of the immunosuppressant tacrolimus in the small intestine: Cytochrome P450, drug interactions, and interindividual variability. *Drug Metab. Dispos*. **23**:1315–1324 (1995).
4. L. M. Mancinelli, L. Frassetto, L. C. Floren, D. Dressler, S. Carrier, I. Bekersky, L. Z. Benet, and U. Christians. The pharmacokinetics and metabolic disposition of tacrolimus: a comparison across ethnic groups. *Clin. Pharmacol. Ther*. **69**:24–31 (2001).
5. P. E. Wallemacqand, and R. K. Verbeeck. Comparative clinical pharmacokinetics of tacrolimus in paediatric and adult patients. *Clin. Pharmacokinet*. **40**:283–295 (2001).
6. R. Venkataramanan, A. Swaminathan, T. Prasad, A. Jain, S. Zuckerman, V. Warty, J. McMichael, J. Lever, G. Burckart, and T. Starzl. Clinical pharmacokinetics of tacrolimus. *Clin. Pharmacokinet*. **29**:404–430 (1995).
7. P. A. Jacobson, C. E. Johnson, N. J. West, and J. A. Foster. Stability of tacrolimus in an extemporaneously compounded oral liquid. *Am. J. Health-Syst. Pharm*. **54**:178–180 (1997).
8. K. Yamashita, T. Nakate, K. Okimoto, A. Ohike, Y. Tokunaga, R. Ibuki, K. Higaki, and T. Kimura. Establishment of new preparation method for solid dispersion formulation of tacrolimus. *Int. J. Pharm*. **267**:79–91 (2003).
9. H. Arima, K. Yunomae, F. Hirayama, and K. Uekama. Contribution of P-glycoprotein to the enhancing effects of dimethyl-beta-cyclodextrin on oral bioavailability of tacrolimus. *J. Pharmacol. Exp. Ther*. **297**:547–555 (2001).
10. H. Arima, K. Yunomae, K. Miyake, T. Irie, F. Hirayama, and K. Uekama. Comparative studies of the enhancing effects of cyclodextrins on the solubility and oral bioavailability of tacrolimus in rats. *J. Pharm. Sci*. **90**:690–701 (2001).
11. M. J. Lee, R. M. Straubinger, and W. J. Jusko. Physicochemical, pharmacokinetic and pharmacodynamic evaluation of liposomal tacrolimus (Fk-506) in rats. *Pharm. Res*. **12**:1055–1059 (1995).
12. S. D. Moffatt, V. McAlister, R. Y. Calne, and S. M. Metcalfe. Potential for improved therapeutic index of FK506 in liposomal formulation demonstrated in a mouse cardiac allograft model. *Transplantation* **67**:1205–1208 (1999).
13. O. Canadas, R. Guerrero, R. Garcia-Canero, G. Orellana, M. Menendez, and C. Casals. Characterization of liposomal tacrolimus in lung surfactant-like phospholipids and evaluation of its immunosuppressive activity. *Biochemistry* **43**:9926–9938 (2004).
14. H. Egawa, S. Maeda, E. Yonemochi, T. Oguchi, K. Yamamoto, and Y. Nakai. Solubility parameter and dissolution behavior of cefalexin powders with different crystallinity. *Chem. Pharm. Bull*. **40**:819–820 (1992).
15. T. Sato, A. Okada, K. Sekiguchi, and Y. Tsuda. Difference in physico-pharmaceutical properties between crystalline and non-crystalline 9,3″-diacetylmidecamycin. *Chem. Pharm. Bull*. **29**:2675–2682 (1981).
16. H. Imaizumi, N. Nambu, and T. Nagai. Pharmaceutical interaction in dosage forms and processing .18. stability and several physical-properties of amorphous and crystalline forms of indomethacin. *Chem. Pharm. Bull*. **28**:2565–2569 (1980).
17. P. Gao, M. E. Guyton, T. H. Huang, J. M. Bauer, K. J. Stefanski, and Q. Lu. Enhanced oral bioavailability of a poorly water soluble drug PNU-91325 by supersaturatable formulations. *Drug Dev. Ind. Pharm*. **30**:221–229 (2004).
18. S. L. Raghavan, B. Kiepfer, A. F. Davis, S. G. Kazarian, and J. Hadgraft. Membrane transport of hydrocortisone acetate from supersaturated solutions; the role of polymers. *Int. J. Pharm*. **221**:95–105 (2001).
19. S. L. Raghavan, A. Trividic, A. F. Davis, and J. Hadgraft. Effect of cellulose polymers on supersaturation and *in vitro* membrane transport of hydrocortisone acetate. *Int. J. Pharm*. **193**:231–237 (2000).
20. J. H. Hu, K. P. Johnston, and R. O. Williams. Stable amorphous danazol nanostructured powders with rapid dissolution rates produced by spray freezing into liquid. *Drug Dev. Ind. Pharm*. **30**:695–704 (2004).
21. J. M. Vaughn, J. T. McConville, M. T. Crisp, R. O. Williams III, and K. P. Johnston. Supersaturation produces high bioavailability of amorphous danazol particles formed by evaporative

precipitation into aqueous solution (EPAS) and spray freezing into liquid(SFL) technologies. *Drug Dev. Ind. Pharm.* **32**:559–567 (2006).
22. K. A. Overhoff, K. P. Johnston, and R. O. Williams. Improvement of dissolution rate of poorly water soluble drugs using a new particle engineering process: Spray freezing into liquid. In S. Svenson (ed), *Polymeric Drug Delivery II: Polymeric Matrices and Drug Particle Engineering*, American Chemical Society, Washington, DC, 2006, pp. 305–319.
23. K. A. Overhoff, J. Engstrom, B. Chen, B. Scherzer, T. E. Milner, K. P. Johnston, and R. O. Williams. Novel ultra-rapid freezing particle engineering process for enhancement of dissolution rates of poorly water soluble drugs. *Eur. J. Pharm. Biopharm.* **65**:57–67 (2006).
24. T. L. Rogers, J. H. Hu, Z. S. Yu, K. P. Johnston, and R. O. Williams III. A novel particle engineering technology: spray-freezing into liquid. *Int. J. Pharm.* **242**:93–100 (2002).
25. J. M. Vaughn, J. T. McConville, D. Burgess, R. L. Talbert, J. I. Peters, R. O. Williams III, and K. P. Johnston. Single dose and multiple dose studies of aerosolized itraconazole nanoparticles. *Eur. J. Pharm. Biopharm.* **63**:95–102 (2005).
26. N. A. Megrab, A. C. Williams, and B. W. Barry. Estradiol permeation through human skin and silastic membrane—effects of propylene-glycol and supersaturation. *J. Control. Release* **36**:277–294 (1995).
27. M. H. Sung, J. S. Kim, W. S. Kim, and I. Hirasawa. Modification of crystal growth mechanism of yttrium oxalate in metastable solution. *J. Cryst. Growth.* **235**:529–540 (2002).
28. S. L. Lawand, and J. B. Kayes. Adsorption of non-ionic water-soluble cellulose polymers at the solid water interface and their effect on suspension stability. *Int. J. Pharm.* **15**:251–260 (1983).
29. S. L. vanRagha, A. Trividic, A. F. Davis, and J. Hadgraft. Crystallization of hydrocortisone acetate: influence of polymers. *Int. J. Pharm.* **212**:213–221 (2001).
30. F. Usui, K. Maeda, A. Kusai, K. Nishimura, and K. Yamamoto. Inhibitory effects of water-soluble polymers on precipitation of RS-8359. *Int. J. Pharm.* **154**:59–66 (1997).
31. H. Suzukiand, and H. Sunada. Influence of water-soluble polymers on the dissolution of nifedipine solid dispersions with combined carriers. *Chem. Pharm. Bull.* **46**:482–487 (1998).
32. A. J. Mackellar, G. Buckton, J. M. Newton, and C. A. Orr. The controlled crystallization of a model powder. 2. Investigation into the mechanism of action of poloxamers in changing crystal properties. *Int. J. Pharm.* **112**:79–85 (1994).
33. K. Ueda, K. Shimojo, T. Shimazaki, I. Kado, and K. Honbo. Solid Dispersion of FR-900506 substance. United States Patent US4,916,138. (1990).
34. T. Nishikawa, H. Hasumi, S. Suzuki, H. Kubo, and H. Ohtani. Kinetic-analysis of molecular interconversion of immunosuppressant Fk506 by high-performance liquid-chromatography. *Pharm. Res.* **10**:1785–1789 (1993).
35. S. Brunauer, P. H. Emmett, and E. Teller. Adsorption of gases in multimolecular layers. *J. Am. Chem. Soc.* **60**:309–319 (1938).
36. J. Dietemann, P. Berthoux, J. P. Gay-Montchamp, M. Batie, and F. Berthoux. Comparison of ELISA method *versus* MEIA method for daily practice in the therapeutic monitoring of tacrolimus. *Nephrol. Dial. Transplant* **16**:2246–2249 (2001).
37. S. Chutimaworapan, G. C. Ritthidej, E. Yonemochi, T. Oguchi, and K. Yamamoto. Effect of water-soluble carriers on dissolution characteristics of nifedipine solid dispersions. *Drug Dev. Ind. Pharm.* **26**:1141–1150 (2000).
38. J. T. McConville, K. A. Overhoff, P. Sinswat, J. M. Vaughn, B. L. Frei, D. S. Burgess, R. L. Talbert, J. I. Peters, K. P. Johnston, and R. O. Williams. Targeted high lung concentrations of itraconazole using nebulized dispersions in a murine model. *Pharm. Res.* **23**:901–911 (2006).
39. S. Tamura, A. Ohike, R. Ibuki, G. L. Amidon, and S. Yamashita. Tacrolimus is a class II low-solubility high-permeability drug: The effect of P-glycoprotein efflux on regional permeability of tacrolimus in rats. *J. Pharm. Sci.* **91**:719–729 (2002).
40. E. Dutkiewiczand, and A. Jakubowska. Effect of electrolytes on the physicochemical behaviour of sodium dodecyl sulphate micelles. *Colloid Polym. Sci.* **280**:1009–1014 (2002).
41. V. V. Khutoryanskiy, G. A. Mun, Z. S. Nurkeeva, and A. V. Dubolazov. pH and salt effects on interpolymer complexation via hydrogen bonding in aqueous solutions. *Polym. Int.* **53**:1382–1387 (2004).
42. N. Pandit, T. Trygstad, S. Croy, M. Bohorquez, and C. Koch. Effect of salts on the micellization, clouding, and solubilization behavior of pluronic F127 solutions. *J. Colloid Interface. Sci.* **222**:213–220 (2000).
43. L. Z. Benet, T. Izumi, Y. C. Zhang, J. A. Silverman, and V. J. Wacher. Intestinal MDR transport proteins and P-450 enzymes as barriers to oral drug delivery. *J. Control. Release* **62**:25–31 (1999).
44. Y. Hashimoto, H. Sasa, M. Shimomura, and K. Inui. Effects of intestinal and hepatic metabolism on the bioavailability of tacrolimus in rats. *Pharm. Res.* **15**:1609–1613 (1998).
45. K. Yokogawa, M. Takahashi, I. Tamai, H. Konishi, M. Nomura, S. Moritani, K. Miyamoto, and A. Tsuji. P-glycoprotein-dependent disposition kinetics of tacrolimus: studies in mdr1a knockout mice. *Pharm. Res.* **16**:1213–1218 (1999).
46. W. L. Chiou, S. M. Chung, and T. C. Wu. Apparent lack of effect of P-glycoprotein on the gastrointestinal absorption of a substrate, tacrolimus, in normal mice. *Pharm. Res.* **17**:205–208 (2000).
47. H. Saitoh, Y. Saikachi, M. Kobayashi, M. Yamaguchi, M. Oda, Y. Yuhki, K. Achiwa, K. Tadano, Y. Takahashi, and B. J. Aungst. Limited interaction between tacrolimus and P-glycoprotein in the rat small intestine. *Eur. J. Pharm. Sci.* **28**:34–42 (2006).
48. A. Kagayama, S. Tanimoto, J. Fujisaki, A. Kaibara, K. Ohara, K. Iwasaki, Y. Hirano, and T. Hata. Oral absorption of Fk506 in rats. *Pharm. Res.* **10**:1446–1450 (1993).
49. J. H. Lin. Species similarities and differences in pharmacokinetics. *Drug Metab. Dispos.* **23**:1008–1021 (1995).